X-ray spectroscopy of low-mass X-ray binaries

Laurence Boirin

Observatoire astronomique de Strasbourg

Artistic impression of a low-mass X-ray binary

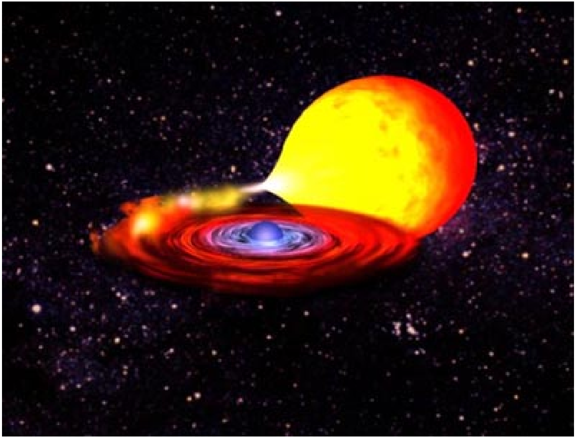

An X-ray binary spectrum (from the past)

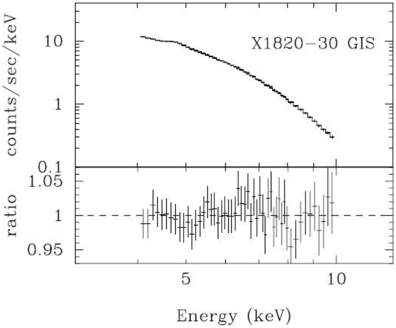

Asai et al. 2000

- continuum emission (bb+powerlaw)

An X-ray binary spectrum (from the past)

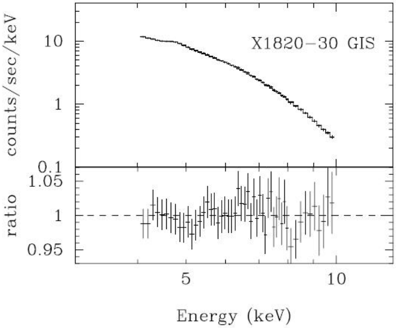

Asai et al. 2000

- continuum emission (bb+powerlaw)
- modified by absorption from elements in the ISM and possibly in the system

Often, an emission line near 6.4 keV

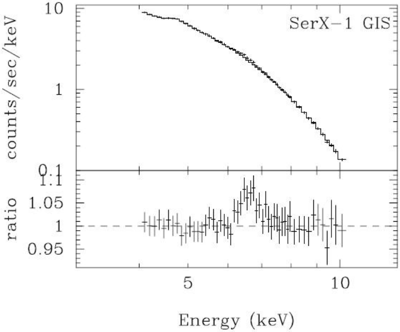

Asai et al. 2000

- Fe K fluorescence

Often, an emission line near 6.4 keV

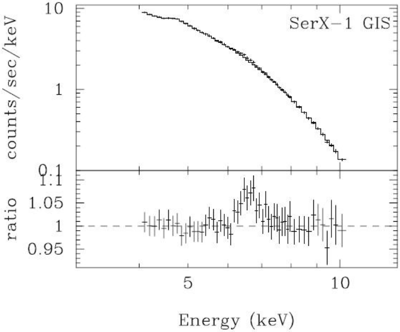

Asai et al. 2000

- Fe K fluorescence
- radiative stabilization following inner-shell photoionization by hard X-ray continuum in a relatively cool and dense medium

Often, an emission line near 6.4 keV

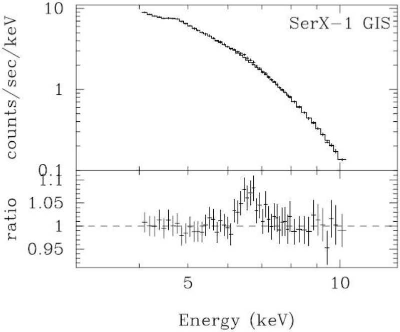

Asai et al. 2000

- Fe K fluorescence
- radiative stabilization following inner-shell photoionization by hard X-ray continuum in a relatively cool and dense medium
- "X-ray reflection"

Often, an emission line near 6.4 keV

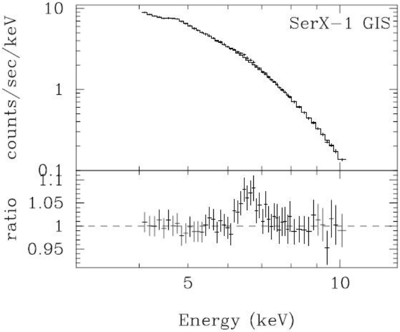

Asai et al. 2000

- Fe K fluorescence
- radiative stabilization following inner-shell photoionization by hard X-ray continuum in a relatively cool and dense medium
- “X-ray reflection”
- often broad

Often, an emission line near 6.4 keV

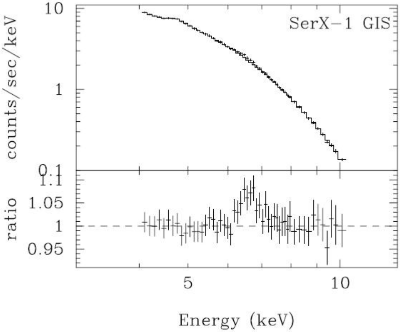

Asai et al. 2000

- Fe K fluorescence
- radiative stabilization following inner-shell photoionization by hard X-ray continuum in a relatively cool and dense medium
- “X-ray reflection”
- often broad
  - » Compton scattering, range of ionization states

Often, an emission line near 6.4 keV

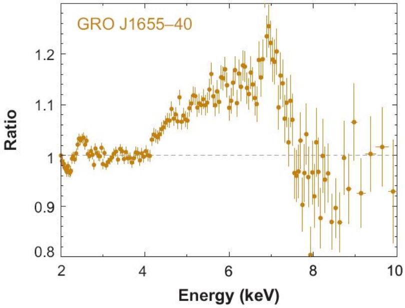

ASCA, Miller et al. 2005

- Fe K fluorescence
- radiative stabilization following inner-shell photoionization by hard X-ray continuum in a relatively cool and dense medium
- “X-ray reflection”
- often broad
  - » Compton scattering, range of ionization states
- broad and asymmetric (red wing) in some BH binaries

Often, an emission line near 6.4 keV

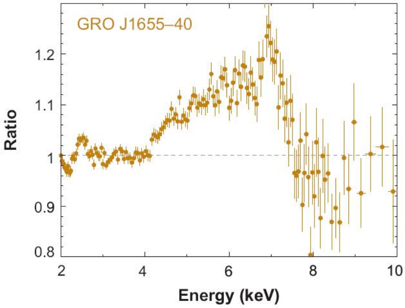

ASCA, Miller et al. 2005

- Fe K fluorescence
- radiative stabilization following inner-shell photoionization by hard X-ray continuum in a relatively cool and dense medium
- “X-ray reflection”
- often broad
  - » Compton scattering, range of ionization states
- broad and asymmetric (red wing) in some BH binaries
  - » relativistically broadened disk-line

What's new in Chandra, XMM and Suzaku spectra?

- imprints from the ISM detected in great detail

What's new in Chandra, XMM and Suzaku spectra?

- imprints from the ISM detected in great detail
  - absorption lines from the hot component of the ISM

What's new in Chandra, XMM and Suzaku spectra?

- imprints from the ISM detected in great detail
  - absorption lines from the hot component of the ISM
  - X-ray absorption fine structures

X-ray aborption fine structures

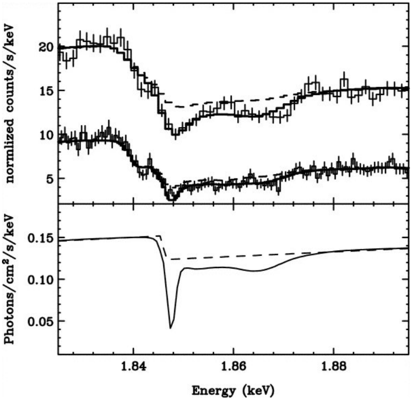

Ueda et al. 2005

- HEG and MEG spectra from a bright X-ray binary showing narrow and broad absorption peaks in the Si K band

X-ray aborption fine structures

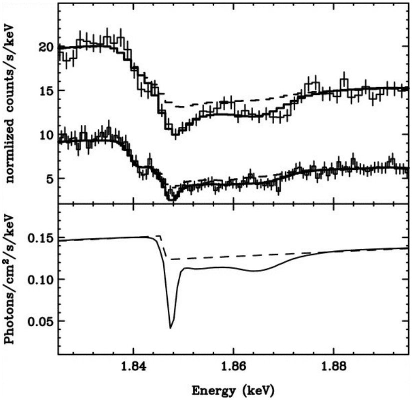

Ueda et al. 2005

- HEG and MEG spectra from a bright X-ray binary showing narrow and broad absorption peaks in the Si K band
- accounted for by X-ray absorption fine structures due to Si in the form of silicates (thick line model)

X-ray aborption fine structures

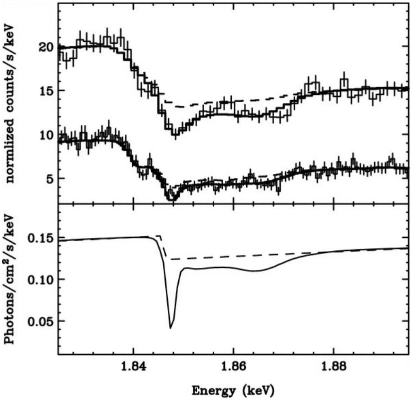

Ueda et al. 2005

- HEG and MEG spectra from a bright X-ray binary showing narrow and broad absorption peaks in the Si K band
- accounted for by X-ray absorption fine structures due to Si in the form of silicates (thick line model)
- rather than a simple absorption edge due to atomic Si (dashed line)

X-ray aborption fine structures

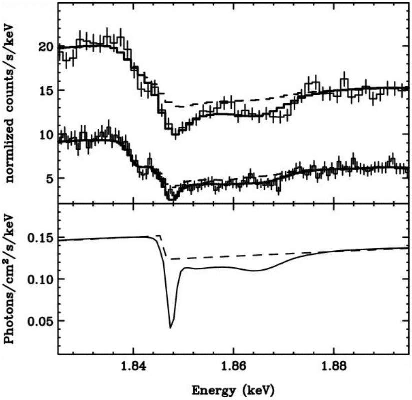

Ueda et al. 2005

- HEG and MEG spectra from a bright X-ray binary showing narrow and broad absorption peaks in the Si K band
- accounted for by X-ray absorption fine structures due to Si in the form of silicates (thick line model)
- rather than a simple absorption edge due to atomic Si (dashed line)

» Constrain the composition of the ISM

What's new in Chandra, XMM and Suzaku spectra?

- imprints from the ISM detected in great detail
  - absorption lines from the hot component of the ISM
  - X-ray absorption fine structures
- broad Fe emission lines still common

What's new in Chandra, XMM and Suzaku spectra?

- imprints from the ISM detected in great detail
  - absorption lines from the hot component of the ISM
  - X-ray absorption fine structures
- broad Fe emission lines still common
- relativistic red wings now reported in NS binaries

Relativistic Fe emission lines in NS binaries

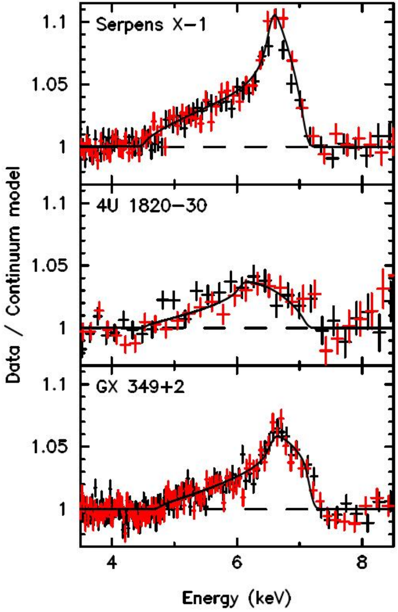

- Suzaku spectral residuals showing asymmetric Fe emission lines fit with a relativistic disk-line model

Relativistic Fe emission lines in NS binaries

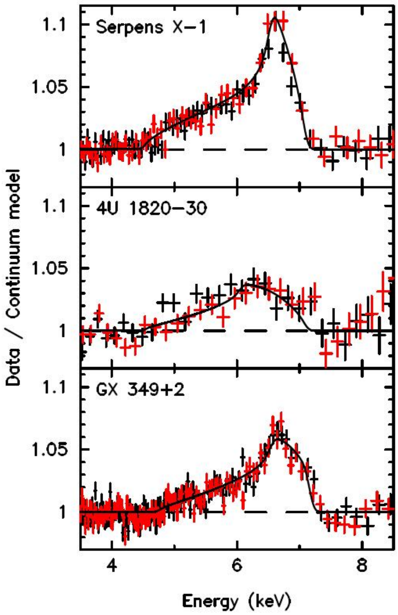

- Suzaku spectral residuals showing asymmetric Fe emission lines fit with a relativistic disk-line model
  - inner radius of the accretion disk and upper-limits on the NS radius

What's new in Chandra, XMM and Suzaku spectra?

- imprints from the ISM detected in great detail
  - absorption lines from the hot component of the ISM
  - X-ray absorption fine structures
- broad Fe emission lines still common
- relativistic red wings now reported in NS binaries
- gravitationaly redshifted absorption lines during bursts from EXO 0748-676, attributed to the NS photosphere

What's new in Chandra, XMM and Suzaku spectra?

- imprints from the ISM detected in great detail
  - absorption lines from the hot component of the ISM
  - X-ray absorption fine structures
- broad Fe emission lines still common
- relativistic red wings now reported in NS binaries
- gravitationaly redshifted absorption lines during bursts from EXO 0748-676, attributed to the NS photosphere
- narrow lines from ionized material located in the X-ray binary

Absorption lines in an **XMM pn** spectrum

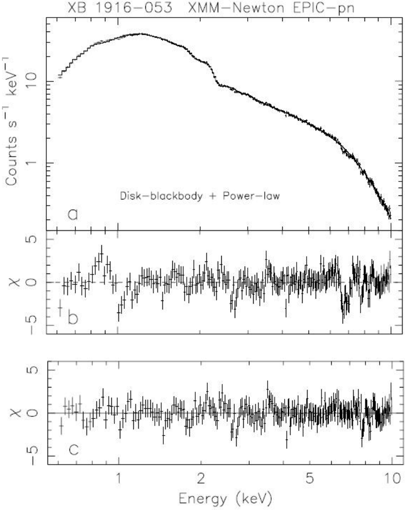

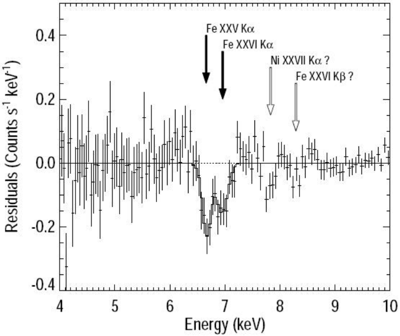

Absorption lines in a **Suzaku XIS** spectrum

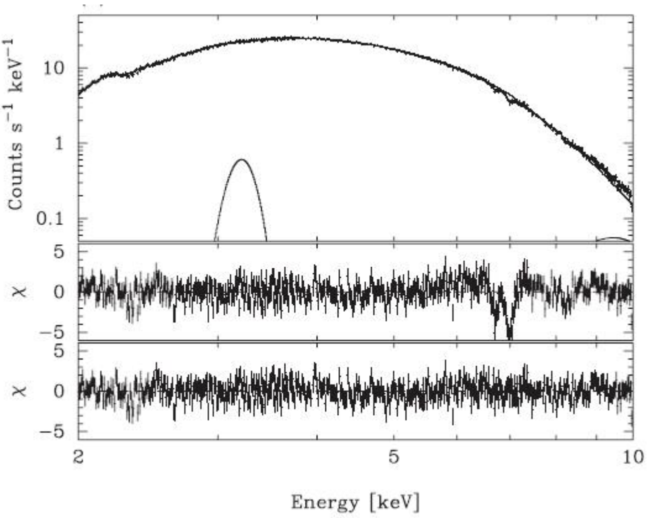

Absorption lines in a **Chandra HEG** spectrum

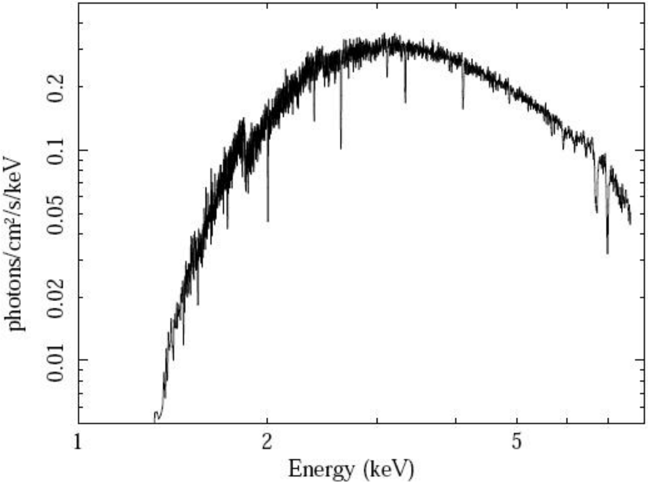

Emission lines in a **Chandra MEG** spectrum

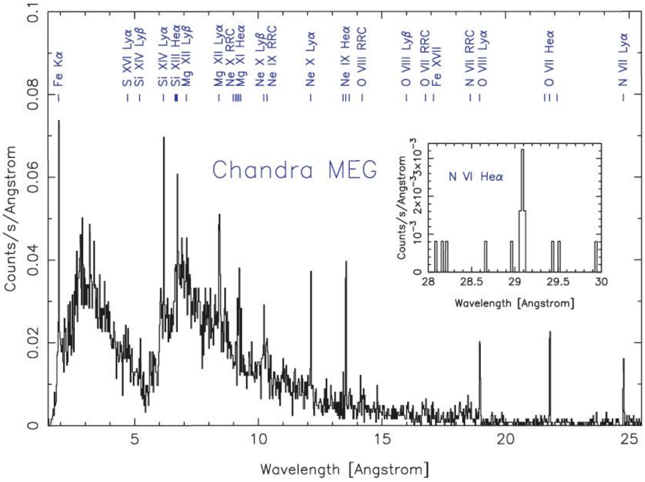

Similar detections in about 25 LMXBs

more frequently in absorption: warm absorbers

[**1**] Kubota et al 2007 [**2**] Di Salvo et al 2005 [**3**] D'Aí et al 2006 [**4**] Miller et al 2006b [**5**] Blum et al 2008 [**6**] Schulz et al 2001 [**7**] Krauss et al 2007 [**8**] Boirin et al 2004 [**9**] Juett and Chakrabarty 2006 [**10**] Iaria et al 2006 [**11**] Díaz Trigo et al 2006 [**12**] Hakala et al 2005 [**13**] Paizis et al 2005 [**14**] Church et al 2005 [**15**] Boirin et al 2005 [**16**] Cottam et al 2001a [**17**] Bonnet-Bidaud et al 2001 [**18**] Homan et al 2003 [**19**] Jimenez-Garate et al 2003 [**20**] van Peet et al 2009 [**21**] Boirin and Parmar 2003 [**22**] Iaria et al 2007a [**23**] Cottam et al 2001b [**24**] Sidoli et al 2001 [**25**] Miller et al 2004 [**26**] Lavagetto et al 2008 [**27**] Hyodo et al 2008 [**28**] Parmar et al 2002 [**29**] Iaria et al 2007b [**30**] Jimenez-Garate et al 2002 [**31**] Jimenez-Garate et al 2005 [**32**] Zane et al 2004 [**33**] Ueda et al 1998 [**34**] Yamaoka et al 2001 [**35**] Bałucińska-Church and Church 2000 [**36**] Miller et al 2006a [**37**] Netzer 2006 [**38**] Miller et al 2008 [**39**] Díaz Trigo et al 2007 [**40**] Sala et al 2007 [**41**] Takahashi et al 2008 [**42**] Kallman et al 2003 [**43**] Schulz et al 2009 [**44**] Brandt and Schulz 2000 [**45**] Schulz and Brandt 2002 [**46**] Iaria et al 2001a [**47**] Iaria et al 2001b [**48**] D'Aí et al 2007 [**49**] Schulz et al 2008 [**50**] Schulz et al 2008 [**51**] Ueda et al 2001 [**52**] Sidoli et al 2002 [**53**] Ueda et al 2004 [**54**] Kotani et al 2000 [**55**] Lee et al 2002 [**56**] Martocchia et al 2006 [**57**] Ueda et al 2009 [**58**] Tiengo et al 2005 [**59**] Paul et al 2005

Identification

- lines associated with electronic transitions (mostly 1s–2p Lyα) in H-like and He-like ions

Identification

- lines associated with electronic transitions (mostly 1s–2p Lyα) in H-like and He-like ions

Ion	-like	Term	Energy (keV)	Wavelength (Å)
O VII	He	$^1P_1$	0.57395	21.602
O VIII	H	$^2P_{1/2}$	0.65349	18.972
		$^2P_{3/2}$	0.65368	18.967
Ne IX	He	$^1P_1$	0.92201	13.447
Ne X	H	$^2P_{1/2}$	1.0215	12.137
		$^2P_{3/2}$	1.0220	12.132
Mg XI	He	$^1P_1$	1.3522	9.1688
Mg XII	H	$^2P_{1/2}$	1.4717	8.4246
		$^2P_{3/2}$	1.4726	8.4192
Al XII	He	$^1P_1$	1.5983	7.7573
Al XIII	H	$^2P_{1/2}$	1.7277	7.1763
		$^2P_{3/2}$	1.7290	7.1709
Si XIII	He	$^1P_1$	1.8650	6.6480
Si XIV	H	$^2P_{1/2}$	2.0043	6.1858
		$^2P_{3/2}$	2.0061	6.1804
S XV	He	$^1P_1$	2.4606	5.0387
S XVI	H	$^2P_{1/2}$	2.6197	4.7328
		$^2P_{3/2}$	2.6227	4.7274
Ar XVII	He	$^1P_1$	3.1398	3.9488
Ar XVIII	H	$^2P_{1/2}$	3.3182	3.7365
		$^2P_{3/2}$	3.3230	3.7311
Ca XIX	He	$^1P_1$	3.9023	3.1772
Ca XX	H	$^2P_{1/2}$	4.1001	3.0239
		$^2P_{3/2}$	4.1075	3.0185
Fe XXV	He	$^1P_1$	6.7004	1.8504
Fe XXVI	H	$^2P_{1/2}$	6.9517	1.7835
		$^2P_{3/2}$	6.9732	1.7780
Ni XXVII	He	$^1P_1$	7.8051	1.5885
Ni XXVIII	H	$^2P_{1/2}$	8.0729	1.5358
		$^2P_{3/2}$	8.1014	1.5304

Identification

- lines associated with electronic transitions (mostly 1s–2p Lyα) in H-like and He-like ions
- Indicate the presence of a highly-ionized plasma in the system

Ion	-like	Term	Energy (keV)	Wavelength (Å)
O VII	He	$^1P_1$	0.57395	21.602
O VIII	H	$^2P_{1/2}$	0.65349	18.972
		$^2P_{3/2}$	0.65368	18.967
Ne IX	He	$^1P_1$	0.92201	13.447
Ne X	H	$^2P_{1/2}$	1.0215	12.137
		$^2P_{3/2}$	1.0220	12.132
Mg XI	He	$^1P_1$	1.3522	9.1688
Mg XII	H	$^2P_{1/2}$	1.4717	8.4246
		$^2P_{3/2}$	1.4726	8.4192
Al XII	He	$^1P_1$	1.5983	7.7573
Al XIII	H	$^2P_{1/2}$	1.7277	7.1763
		$^2P_{3/2}$	1.7290	7.1709
Si XIII	He	$^1P_1$	1.8650	6.6480
Si XIV	H	$^2P_{1/2}$	2.0043	6.1858
		$^2P_{3/2}$	2.0061	6.1804
S XV	He	$^1P_1$	2.4606	5.0387
S XVI	H	$^2P_{1/2}$	2.6197	4.7328
		$^2P_{3/2}$	2.6227	4.7274
Ar XVII	He	$^1P_1$	3.1398	3.9488
Ar XVIII	H	$^2P_{1/2}$	3.3182	3.7365
		$^2P_{3/2}$	3.3230	3.7311
Ca XIX	He	$^1P_1$	3.9023	3.1772
Ca XX	H	$^2P_{1/2}$	4.1001	3.0239
		$^2P_{3/2}$	4.1075	3.0185
Fe XXV	He	$^1P_1$	6.7004	1.8504
Fe XXVI	H	$^2P_{1/2}$	6.9517	1.7835
		$^2P_{3/2}$	6.9732	1.7780
Ni XXVII	He	$^1P_1$	7.8051	1.5885
Ni XXVIII	H	$^2P_{1/2}$	8.0729	1.5358
		$^2P_{3/2}$	8.1014	1.5304

H-like

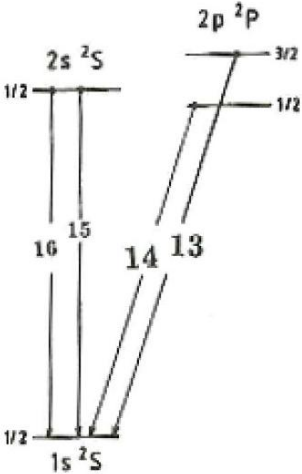

- resonance line either in absorption or in emission

H-like

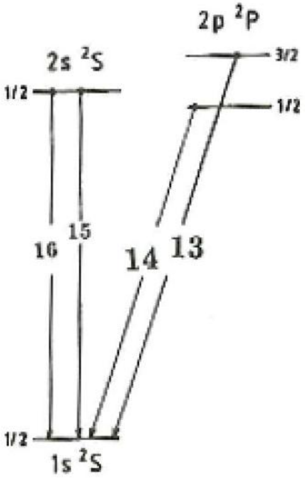

- resonance line either in absorption or in emission
- the 2 components of the resonance line are unresolved

He-like

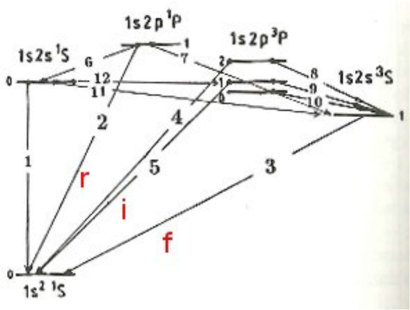

- in absorption: the resonance line

He-like

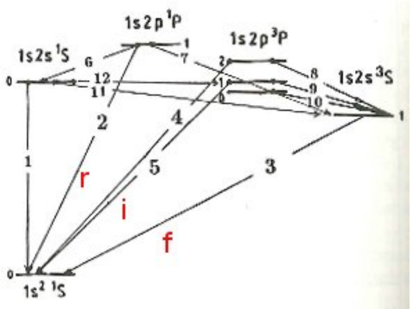

- in absorption: the resonance line
- in emission: the “triplet” of resonance, intercombination and forbidden lines

He-like

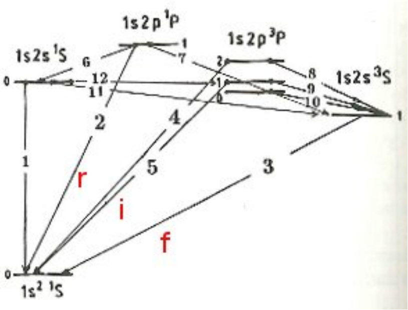

- in absorption: the resonance line
- in emission: the “triplet” of resonance, intercombination and forbidden lines
- the relative strength of the triplet components depends on the physical conditions of the plasma

He-like

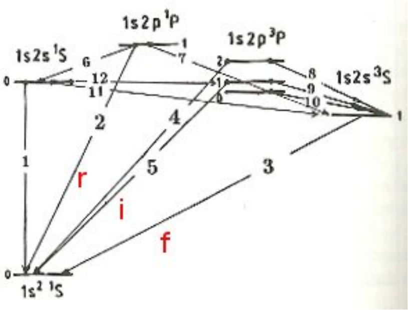

- in absorption: the resonance line
- in emission: the “triplet” of resonance, intercombination and forbidden lines
- the relative strength of the triplet components depends on the physical conditions of the plasma
    - ionization mechanism: collisional or photo-ionization

He-like

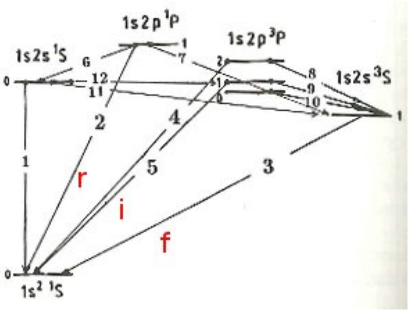

- in absorption: the resonance line
- in emission: the "triplet" of resonance, intercombination and forbidden lines
- the relative strength of the triplet components depends on the physical conditions of the plasma
  - ionization mechanism: collisional or photo-ionization
  - density

He-like

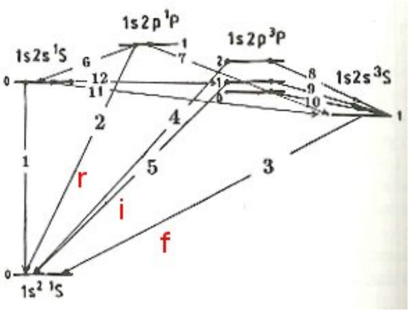

- in absorption: the resonance line
- in emission: the "triplet" of resonance, intercombination and forbidden lines
- the relative strength of the triplet components depends on the physical conditions of the plasma
  - ionization mechanism: collisional or photo-ionization
  - density
  - temperature

He-like

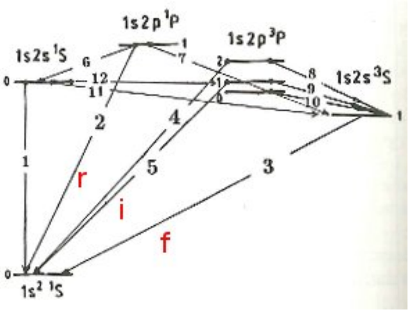

- in absorption: the resonance line
- in emission: the “triplet” of resonance, intercombination and forbidden lines
- the relative strength of the triplet components depends on the physical conditions of the plasma
  - ionization mechanism: collisional or photo-ionization
  - density
  - temperature

see e.g. Porquet and Dubau 2000

Ionization mechanism in LMXBs?

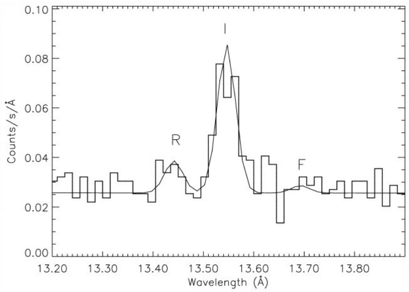

Ne IX *triplet in 2A 1822-371, Cottam et al. 2001*

- He-like triplets tend to show:

Ionization mechanism in LMXBs?

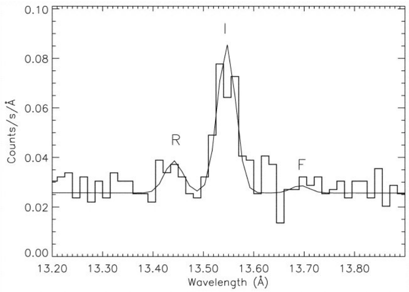

Ne IX *triplet in 2A 1822-371, Cottam et al. 2001*

- He-like triplets tend to show:
  - a bright intercombination line

Ionization mechanism in LMXBs?

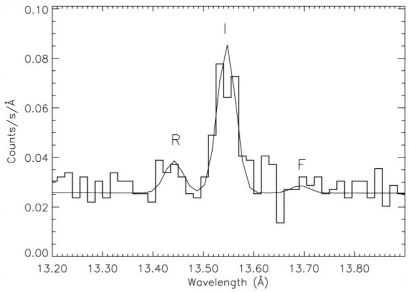

Ne IX *triplet in 2A 1822-371, Cottam et al. 2001*

- He-like triplets tend to show:
  - a bright intercombination line
  - a weak resonance line

Ionization mechanism in LMXBs?

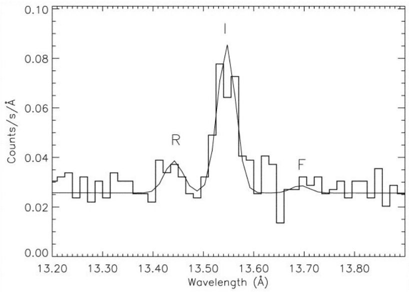

Ne IX *triplet in 2A 1822-371, Cottam et al. 2001*

- He-like triplets tend to show:
  - a bright intercombination line
  - a weak resonance line
  - no forbidden line

Ionization mechanism in LMXBs?

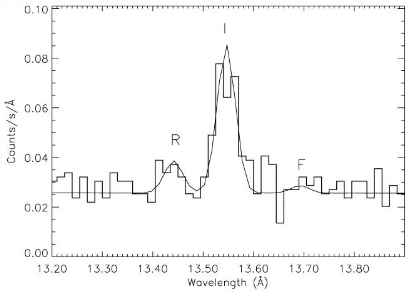

Ne IX *triplet in 2A 1822-371, Cottam et al. 2001*

- He-like triplets tend to show:
  - a bright intercombination line
  - a weak resonance line
  - no forbidden line
- indicative of a recombining (photoionized) plasma

Radiative recombination continua (RRC)

Models, Kahn 2000

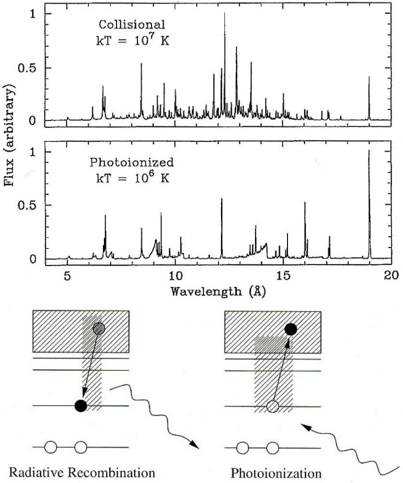

- a feature characteristic of photoionized plasma

Radiative recombination continua (RRC)

Models, Kahn 2000

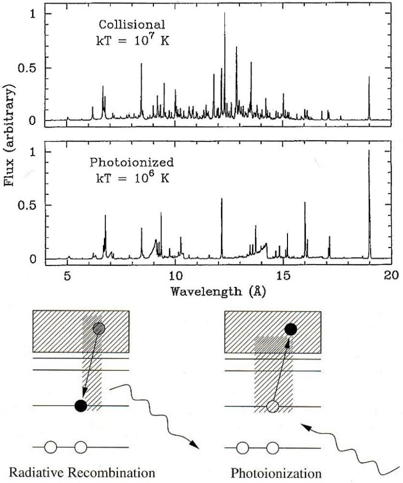

- a feature characteristic of photoionized plasma
- its width is a direct measure of the plasma temperature

Radiative recombination continua (RRC)

Models, Kahn 2000

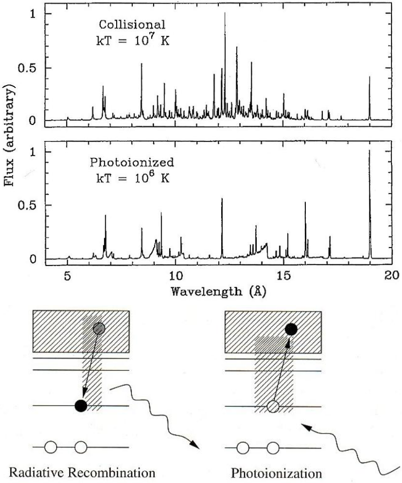

- a feature characteristic of photoionized plasma
- its width is a direct measure of the plasma temperature
- detected from 3 LMXBs

Radiative recombination continua (RRC)

Models, Kahn 2000

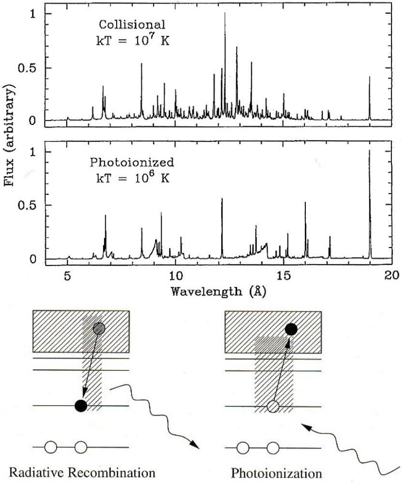

- a feature characteristic of photoionized plasma
- its width is a direct measure of the plasma temperature
- detected from 3 LMXBs

» kT $\lesssim$ 20 eV

Radiative recombination continua (RRC)

Models, Kahn 2000

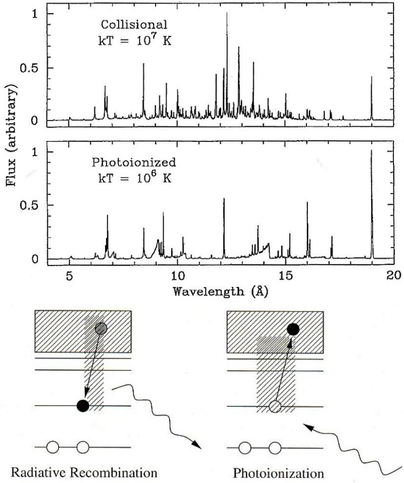

- a feature characteristic of photoionized plasma
- its width is a direct measure of the plasma temperature
- detected from 3 LMXBs

» kT $\lesssim$ 20 eV

» Photoionization is the dominant ionization mechanism

Other supports to photoionization

Suzaku spectra covering an outburst decay

Kubota et al. 2007

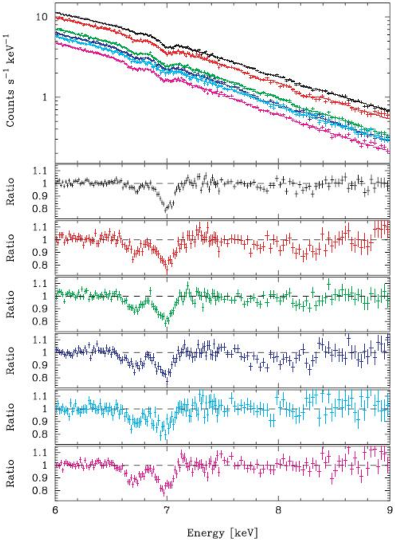

- presence of a strong ionizing source (the X-ray continuum!)

Other supports to photoionization

Suzaku spectra covering an outburst decay

Kubota et al. 2007

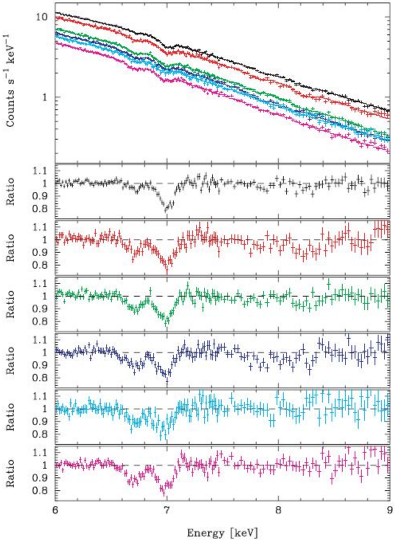

- presence of a strong ionizing source (the X-ray continuum!)
- evidence for decrease of the ionization state with the X-ray luminosity

Other supports to photoionization

Suzaku spectra covering an outburst decay

Kubota et al. 2007

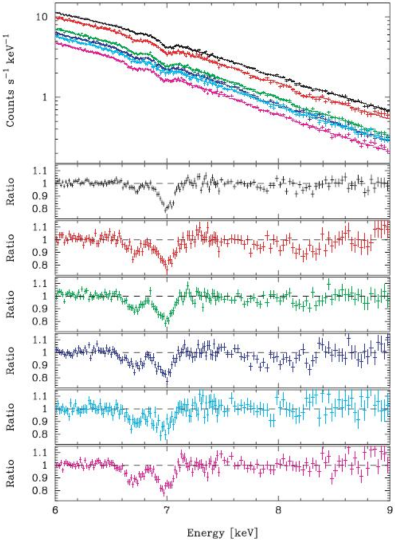

- presence of a strong ionizing source (the X-ray continuum!)
- evidence for decrease of the ionization state with the X-ray luminosity

Other supports to photoionization

Suzaku spectra covering an outburst decay

Kubota et al. 2007

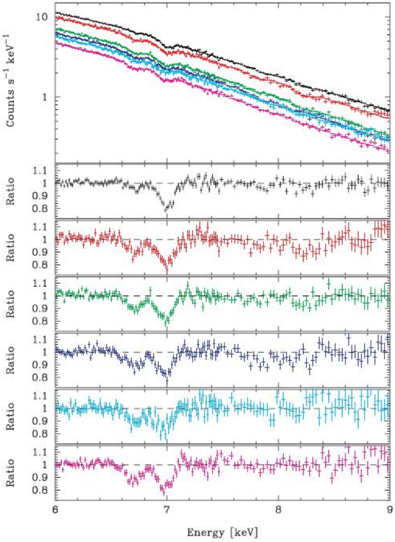

- presence of a strong ionizing source (the X-ray continuum!)
- evidence for decrease of the ionization state with the X-ray luminosity
- See however the talk by E. Costantini: collisionaly ionized plasma in EXO 0748-676.

Other supports to photoionization

Suzaku spectra covering an outburst decay

Kubota et al. 2007

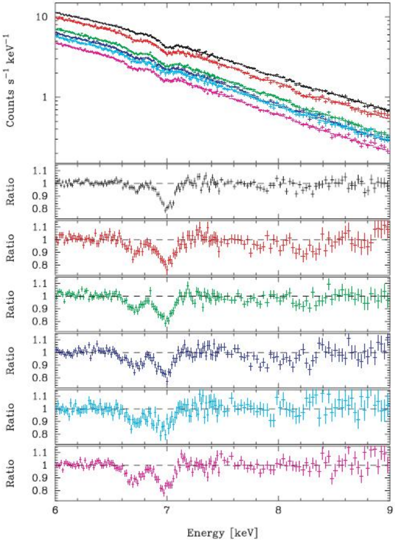

- presence of a strong ionizing source (the X-ray continuum!)
- evidence for decrease of the ionization state with the X-ray luminosity

- See however the talk by E. Costantini: collisionaly ionized plasma in EXO 0748-676.
- Hybrid plasmas

Where is the ionized plasma located?

LMXBs with spectral signatures of a warm absorber/emitter

Source
● 4U 1630-47
○ 4U 1705-44
○ 4U 1728-34
● H1743-322
○ 4U 1626-67
○ 4U 1916-05
○ 1E 1603.6+2600
○ IGR J00291+5934
○ 4U 1323-62
○ EXO 0748-676
○ 4U 1254-69
○ 4U 1746-37
○ 2A 1822-371
○ MXB 1659-298
● XTE J1650-500
○ LMC X-2
○ AX J1745.6-2901
○ 4U 1624-49
○ Her X-1
● GX 339-4
● GRO J1655-40
○ 2S 0921-630
○ Cyg X-2
○ Cir X-1
○ GX 13+1
● GRS 1915+105

LMXBs with spectral signatures of a warm absorber/emitter

Source	P_{orb}
• 4U 1630-47	
○ 4U 1705-44	1–10 h[h]
○ 4U 1728-34	
• H1743-322	
○ 4U 1626-67	0.69 h
○ 4U 1916-05	0.83 h
○ 1E 1603.6+2600	1.85 h
○ IGR J00291+5934	2.45 h
○ 4U 1323-62	2.9 h
○ EXO 0748-676	3.82 h
○ 4U 1254-69	3.93 h
○ 4U 1746-37	5.16 h
○ 2A 1822-371	5.57 h
○ MXB 1659-298	7.11 h
• XTE J1650-500	7.63 h
○ LMC X-2	8.16 h
○ AX J1745.6-2901	8.4 h
○ 4U 1624-49	20.89 h
○ Her X-1	1.70 d
• GX 339-4	1.76 d[m]
• GRO J1655-40	2.62 d
○ 2S 0921-630	9.01 d
○ Cyg X-2	9.84 d
○ Cir X-1	16.6 d
○ GX 13+1	24.06 d
• GRS 1915+105	33.5 d

LMXBs with spectral signatures of a warm absorber/emitter

Source	P_{orb}	Type
• 4U 1630-47		T, R
○ 4U 1705-44	1–10 h^o	B, A, R
○ 4U 1728-34		B, A, R
• H1743-322		T, M, R
○ 4U 1626-67	0.69 h	P
○ 4U 1916-05	0.83 h	B, A
○ 1E 1603.6+2600	1.85 h	B
○ IGR J00291+5934	2.45 h	T, msP, R
○ 4U 1323-62	2.9 h	B
○ EXO 0748-676	3.82 h	T, B
○ 4U 1254-69	3.93 h	B
○ 4U 1746-37	5.16 h	G, B, A
○ 2A 1822-371	5.57 h	P
○ MXB 1659-298	7.11 h	T, B
• XTE J1650-500	7.63 h	T, R
○ LMC X-2	8.16 h	Z
○ AX J1745.6-2901	8.4 h	T, B
○ 4U 1624-49	20.89 h	
○ Her X-1	1.70 d	P
• GX 339-4	1.76 d^t	T, M, R
• GRO J1655-40	2.62 d	T, M, R
○ 2S 0921-630	9.01 d	
○ Cyg X-2	9.84 d	B, Z, R
○ Cir X-1	16.6 d	T, B, A(Z), M, R
○ GX 13+1	24.06 d	B, A(Z), R
• GRS 1915+105	33.5 d	T, M, R

LMXBs with spectral signatures of a warm absorber/emitter

Source	P_{orb}	Type	D
• 4U 1630-47		T, R	D
○ 4U 1705-44	1–10 h[v]	B, A, R	[w]
○ 4U 1728-34		B, A, R	
• H1743-322		T, M, R	D[y]
○ 4U 1626-67	0.69 h	P	
○ 4U 1916-05	0.83 h	B, A	D
○ 1E 1603.6+2600	1.85 h	B	ADC
○ IGR J00291+5934	2.45 h	T, msP, R	
○ 4U 1323-62	2.9 h	B	D
○ EXO 0748-676	3.82 h	T, B	D, E
○ 4U 1254-69	3.93 h	B	D
○ 4U 1746-37	5.16 h	G, B, A	D
○ 2A 1822-371	5.57 h	P	E (ADC)
○ MXB 1659-298	7.11 h	T, B	D, E
• XTE J1650-500	7.63 h	T, R	
○ LMC X-2	8.16 h	Z	
○ AX J1745.6-2901	8.4 h	T, B	D[z]
○ 4U 1624-49	20.89 h		D
○ Her X-1	1.70 d	P	D, E
• GX 339-4	1.76 d	T, M, R	
• GRO J1655-40	2.62 d	T, M, R	D
○ 2S 0921-630	9.01 d		D, E (ADC)
○ Cyg X-2	9.84 d	B, Z, R	D
○ Cir X-1	16.6 d	T, B, A(Z), M, R	D
○ GX 13+1	24.06 d	B, A(Z), R	
• GRS 1915+105	33.5 d	T, M, R	D

LMXBs with spectral signatures of a warm absorber/emitter

Source	P_{orb}	Type	D	i
• 4U 1630-47		T, R	D	
○ 4U 1705-44	1–10 h	B, A, R		55–84
○ 4U 1728-34		B, A, R		$\sim$50
• H1743-322		T, M, R	D	
○ 4U 1626-67	0.69 h	P		$\lesssim$ 33
○ 4U 1916-05	0.83 h	B, A	D	60–79
○ 1E 1603.6+2600	1.85 h	B	ADC	
○ IGR J00291+5934	2.45 h	T, msP, R		
○ 4U 1323-62	2.9 h	B	D	
○ EXO 0748-676	3.82 h	T, B	D, E	75–82
○ 4U 1254-69	3.93 h	B	D	68–73
○ 4U 1746-37	5.16 h	G, B, A	D	
○ 2A 1822-371	5.57 h	P	E (ADC)	81–84
○ MXB 1659-298	7.11 h	T, B	D, E	
• XTE J1650-500	7.63 h	T, R		$>$50$\pm$3
○ LMC X-2	8.16 h	Z		
○ AX J1745.6-2901	8.4 h	T, B	D	
○ 4U 1624-49	20.89 h		D	
○ Her X-1	1.70 d	P	D, E	
• GX 339-4	1.76 d	T, M, R		15
• GRO J1655-40	2.62 d	T, M, R	D	70.2
○ 2S 0921-630	9.01 d		D, E (ADC)	
○ Cyg X-2	9.84 d	B, Z, R	D	
○ Cir X-1	16.6 d	T, B, A(Z), M, R	D	
○ GX 13+1	24.06 d	B, A(Z), R		
• GRS 1915+105	33.5 d	T, M, R	D	66

LMXBs with spectral signatures of a warm absorber/emitter

Source	P_{orb}	Type	D	i	Emission lines	Absorption
• 4U 1630-47		T, R	D			
◦ 4U 1705-44	1–10 h	B, A, R		55–84	3σ	
◦ 4U 1728-34		B, A, R		$\sim$50		
• H1743-322		T, M, R	D			
◦ 4U 1626-67	0.69 h	P		≤ 33		
◦ 4U 1916-05	0.83 h	B, A	D	60–79		
◦ 1E 1603.6+2600	1.85 h	B	ADC		$\surd$	
◦ IGR J00291+5934	2.45 h	T, msP, R			3σ	
◦ 4U 1323-62	2.9 h	B	D			
◦ EXO 0748-676	3.82 h	T, B	D, E	75–82	$\surd$	
◦ 4U 1254-69	3.93 h	B	D	68–73		
◦ 4U 1746-37	5.16 h	G, B, A	D			
◦ 2A 1822-371	5.57 h	P	E (ADC)	81–84	$\surd$	
◦ MXB 1659-298	7.11 h	T, B	D, E			
• XTE J1650-500	7.63 h	T, R		$>50\pm3$		
◦ LMC X-2	8.16 h	Z			$\surd$	
◦ AX J1745.6-2901	8.4 h	T, B	D			
◦ 4U 1624-49	20.89 h		D			
◦ Her X-1	1.70 d	P	D, E		$\surd$	
• GX 339-4	1.76 d	T, M, R		15		
• GRO J1655-40	2.62 d	T, M, R	D	70.2		
◦ 2S 0921-630	9.01 d		D, E (ADC)		$\surd$	
◦ Cyg X-2	9.84 d	B, Z, R	D		$\surd$	
◦ Cir X-1	16.6 d	T, B, A(Z), M, R	D		$\surd$	
◦ GX 13+1	24.06 d	B, A(Z), R				
• GRS 1915+105	33.5 d	T, M, R	D	66		

LMXBs with spectral signatures of a warm absorber/emitter

Source	P_{orb}	Type	D	i	Emission		Absorption
					lines	RRC	
• 4U 1630-47		T, R	D				
∘ 4U 1705-44	1–10 h	B, A, R		55–84	3σ		
∘ 4U 1728-34		B, A, R		$\sim$50			
• H1743-322		T, M, R	D				
∘ 4U 1626-67	0.69 h	P		$\lesssim 33$			
∘ 4U 1916-05	0.83 h	B, A	D	60–79			
∘ 1E 1603.6+2600	1.85 h	B	ADC		$\surd$		
∘ IGR J00291+5934	2.45 h	T, msP, R			3σ		
∘ 4U 1323-62	2.9 h	B	D				
∘ EXO 0748-676	3.82 h	T, B	D, E	75–82	$\surd$	$\surd$	
∘ 4U 1254-69	3.93 h	B	D	68–73			
∘ 4U 1746-37	5.16 h	G, B, A	D				
∘ 2A 1822-371	5.57 h	P	E (ADC)	81–84	$\surd$	$\surd$	
∘ MXB 1659-298	7.11 h	T, B	D, E				
• XTE J1650-500	7.63 h	T, R		$>50\pm3$			
∘ LMC X-2	8.16 h	Z			$\surd$		
∘ AX J1745.6-2901	8.4 h	T, B	D				
∘ 4U 1624-49	20.89 h		D				
∘ Her X-1	1.70 d	P	D, E		$\surd$	$\surd$	
• GX 339-4	1.76 d	T, M, R		15			
• GRO J1655-40	2.62 d	T, M, R	D	70.2			
∘ 2S 0921-630	9.01 d		D, E (ADC)		$\surd$		
∘ Cyg X-2	9.84 d	B, Z, R	D		$\surd$		
∘ Cir X-1	16.6 d	T, B, A(Z), M, R	D		$\surd$		
∘ GX 13+1	24.06 d	B, A(Z), R					
• GRS 1915+105	33.5 d	T, M, R	D	66			

LMXBs with spectral signatures of a warm absorber/emitter

Source	P_{orb}	Type	D	i	Emission lines	RRC	Absorption lines
• 4U 1630-47		T, R	D				$\surd$
○ 4U 1705-44	1–10 h	B, A, R		55–84	3σ		
○ 4U 1728-34		B, A, R		$\sim$50			
• H1743-322		T, M, R	D				$\surd$
○ 4U 1626-67	0.69 h	P		$\lesssim 33$			
○ 4U 1916-05	0.83 h	B, A	D	60–79			$\surd$
○ 1E 1603.6+2600	1.85 h	B	ADC		$\surd$		
○ IGR J00291+5934	2.45 h	T, msP, R			3σ		
○ 4U 1323-62	2.9 h	B	D				$\surd$
○ EXO 0748-676	3.82 h	T, B	D, E	75–82	$\surd$	$\surd$	$\surd$
○ 4U 1254-69	3.93 h	B	D	68–73			$\surd$
○ 4U 1746-37	5.16 h	G, B, A	D				3σ
○ 2A 1822-371	5.57 h	P	E (ADC)	81–84	$\surd$	$\surd$	
○ MXB 1659-298	7.11 h	T, B	D, E				$\surd$
• XTE J1650-500	7.63 h	T, R		$>50\pm3$			$\surd$
○ LMC X-2	8.16 h	Z			$\surd$		
○ AX J1745.6-2901	8.4 h	T, B	D				$\surd$
○ 4U 1624-49	20.89 h		D				$\surd$
○ Her X-1	1.70 d	P	D, E		$\surd$	$\surd$	
• GX 339-4	1.76 d	T, M, R		15			$\surd$
• GRO J1655-40	2.62 d	T, M, R	D	70.2			$\surd$
○ 2S 0921-630	9.01 d		D, E (ADC)		$\surd$		
○ Cyg X-2	9.84 d	B, Z, R	D		$\surd$		
○ Cir X-1	16.6 d	T, B, A(Z), M, R	D		$\surd$		$\surd$
○ GX 13+1	24.06 d	B, A(Z), R					$\surd$
• GRS 1915+105	33.5 d	T, M, R	D	66			$\surd$

LMXBs with spectral signatures of a warm absorber/emitter

Source	P_{orb}	Type	D	i	Emission		Absorption		
					lines	RRC	lines	edges	Comm
• 4U 1630-47		T, R	D				$\surd$		
◦ 4U 1705-44	1–10 h	B, A, R		55–84	3σ				
◦ 4U 1728-34		B, A, R		$\sim$50				$\surd$	
• H1743-322		T, M, R	D				$\surd$		
◦ 4U 1626-67	0.69 h	P		$\lesssim 33$					Dop. p
◦ 4U 1916-05	0.83 h	B, A	D	60–79			$\surd$	$\surd$	
◦ 1E 1603.6+2600	1.85 h	B	ADC		$\surd$				
◦ IGR J00291+5934	2.45 h	T, msP, R			3σ			3σ	
◦ 4U 1323-62	2.9 h	B	D				$\surd$		
◦ EXO 0748-676	3.82 h	T, B	D, E	75–82	$\surd$	$\surd$	$\surd$	$\surd$	
◦ 4U 1254-69	3.93 h	B	D	68–73			$\surd$		
◦ 4U 1746-37	5.16 h	G, B, A	D				3σ		
◦ 2A 1822-371	5.57 h	P	E (ADC)	81–84	$\surd$	$\surd$			
◦ MXB 1659-298	7.11 h	T, B	D, E				$\surd$		
• XTE J1650-500	7.63 h	T, R		$>50\pm3$			$\surd$		
◦ LMC X-2	8.16 h	Z			$\surd$				
◦ AX J1745.6-2901	8.4 h	T, B	D				$\surd$	$\surd$	
◦ 4U 1624-49	20.89 h		D				$\surd$		
◦ Her X-1	1.70 d	P	D, E		$\surd$	$\surd$		$\surd$	
• GX 339-4	1.76 d	T, M, R		15			$\surd$		
• GRO J1655-40	2.62 d	T, M, R	D	70.2			$\surd$		
◦ 2S 0921-630	9.01 d		D, E (ADC)		$\surd$				
◦ Cyg X-2	9.84 d	B, Z, R	D		$\surd$				
◦ Cir X-1	16.6 d	T, B, A(Z), M, R	D		$\surd$		$\surd$		P-Cyg
◦ GX 13+1	24.06 d	B, A(Z), R					$\surd$		
• GRS 1915+105	33.5 d	T, M, R	D	66			$\surd$		

X-ray orbital variability as a function of inclination

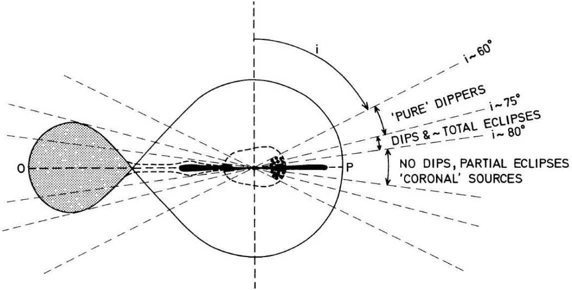

Frank et al. 1987

X-ray orbital variability as a function of inclination

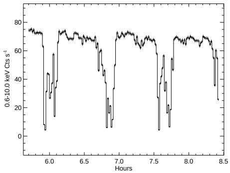

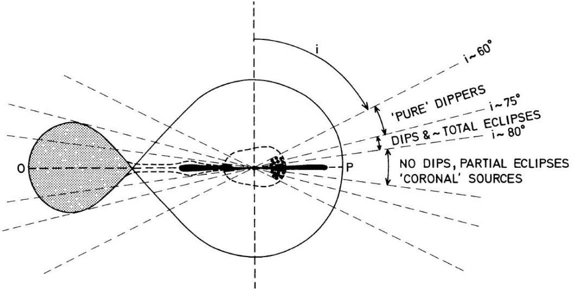

Frank et al. 1987

X-ray orbital variability as a function of inclination

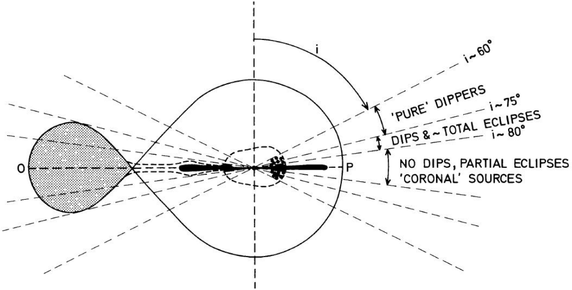

Frank et al. 1987

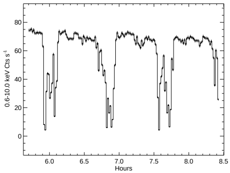

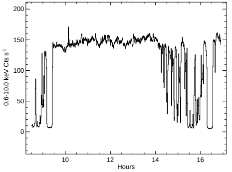

X-ray orbital variability as a function of inclination

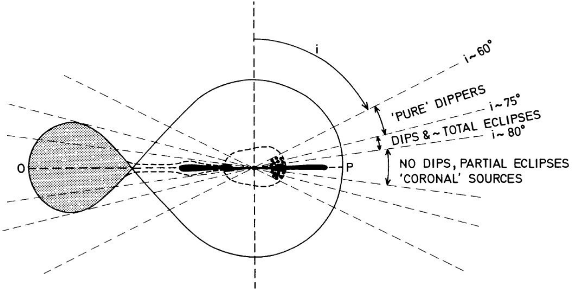

Frank et al. 1987

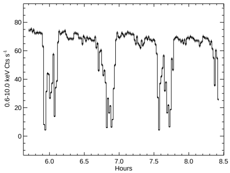

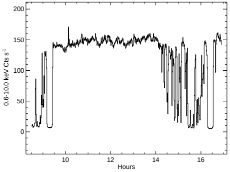

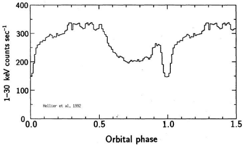

Where is the ionized plasma located?

Where is the ionized plasma located?

- in a flat geometry above the disk

Where is the ionized plasma located?

- in a flat geometry above the disk
- Distance from the ionizing source estimated from the ionization parameter, consistent with being $\lesssim$ the disk size.

Where is the ionized plasma located?

- in a flat geometry above the disk
- Distance from the ionizing source estimated from the ionization parameter, consistent with being $\lesssim$ the disk size.
- Other properties of the plasma

Where is the ionized plasma located?

- in a flat geometry above the disk
- Distance from the ionizing source estimated from the ionization parameter, consistent with being $\lesssim$ the disk size.
- Other properties of the plasma
  - $\log \xi \sim 3$–4

Where is the ionized plasma located?

- in a flat geometry above the disk
- Distance from the ionizing source estimated from the ionization parameter, consistent with being $\lesssim$ the disk size.
- Other properties of the plasma
  - $\log \xi \sim$ 3–4
  - two values of $\log \xi$ required in some cases

Where is the ionized plasma located?

- in a flat geometry above the disk
- Distance from the ionizing source estimated from the ionization parameter, consistent with being $\lesssim$ the disk size.
- Other properties of the plasma
  - $\log \xi \sim$ 3–4
  - two values of $\log \xi$ required in some cases
  - range of ionization?

Where is the ionized plasma located?

- in a flat geometry above the disk
- Distance from the ionizing source estimated from the ionization parameter, consistent with being $\lesssim$ the disk size.
- Other properties of the plasma
  - $\log \xi \sim$ 3–4
  - two values of $\log \xi$ required in some cases
  - range of ionization?
  - indications for the more ionized species being closer to the compact object

Where is the ionized plasma located?

- in a flat geometry above the disk
- Distance from the ionizing source estimated from the ionization parameter, consistent with being $\lesssim$ the disk size.
- Other properties of the plasma
  - $\log \xi \sim$ 3–4
  - two values of $\log \xi$ required in some cases
  - range of ionization?
  - indications for the more ionized species being closer to the compact object
  - vertical stratification also proposed *Jimenez-Garate et al. 2003*

Phase dependence in an ADC source

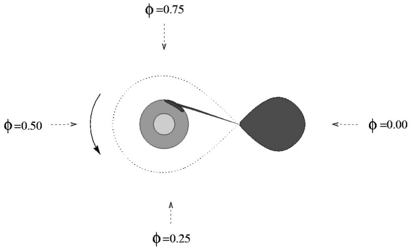

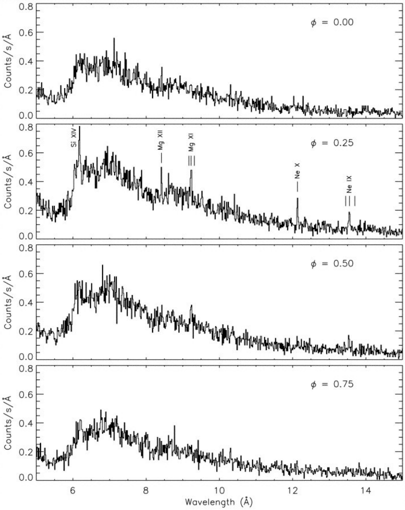

Phase dependence in dippers

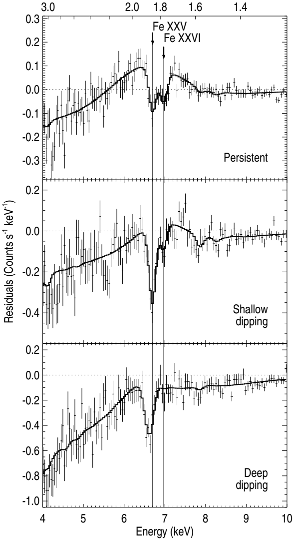

- the properties of the warm absorber do not change as a function of phase during persistent emission

Phase dependence in dippers

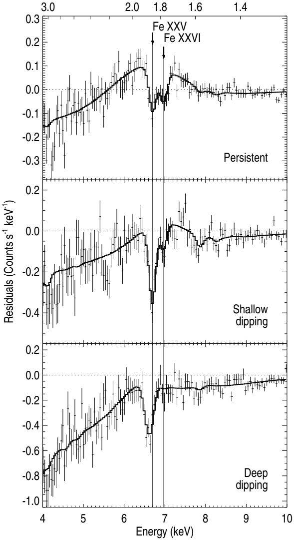

- the properties of the warm absorber do not change as a function of phase during persistent emission
- but do during dipping

Phase dependence in dippers

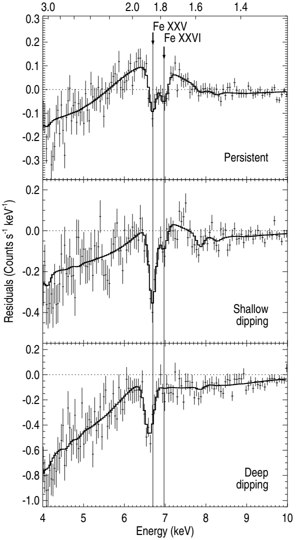

- the properties of the warm absorber do not change as a function of phase during persistent emission
- but do during dipping
  - ionization stage decreases

Phase dependence in dippers

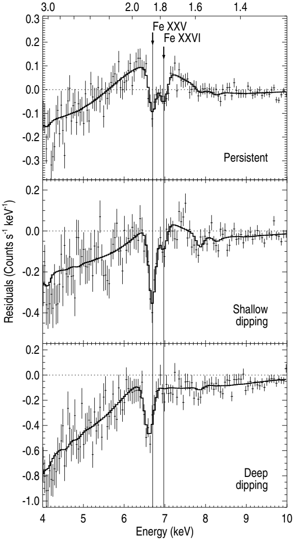

- the properties of the warm absorber do not change as a function of phase during persistent emission
- but do during dipping
  - ionization stage decreases
  - column density increases

Spectral changes during dips

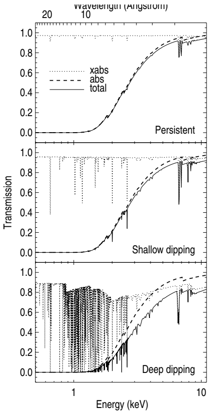

Boirin et al. 2005, Diaz Trigo et al. 2006.

The changes in the properties of the warm absorber combined with an increase of the column density of a neutral absorber can explain the overall (lines and continuum) spectral changes observed during dips from all dippers.

Spectral changes during dips

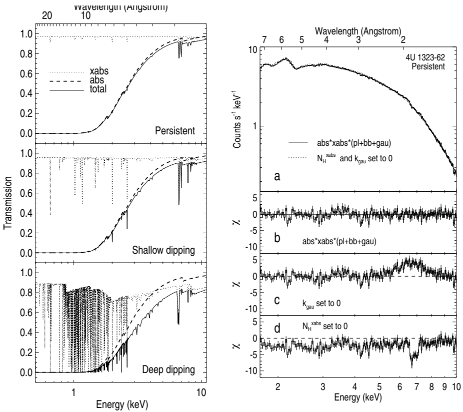

Boirin et al. 2005, Diaz Trigo et al. 2006.

The changes in the properties of the warm absorber combined with an increase of the column density of a neutral absorber can explain the overall (lines and continuum) spectral changes observed during dips from all dippers.

Spectral changes during dips

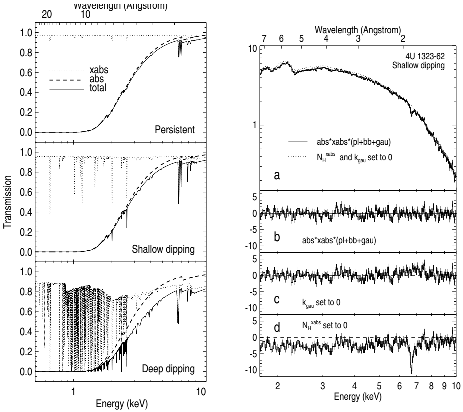

Boirin et al. 2005, Diaz Trigo et al. 2006.

The changes in the properties of the warm absorber combined with an increase of the column density of a neutral absorber can explain the overall (lines and continuum) spectral changes observed during dips from all dippers.

Spectral changes during dips

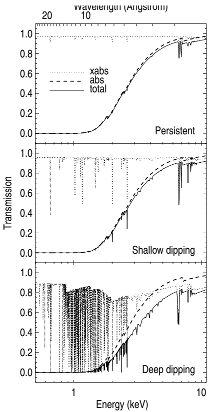

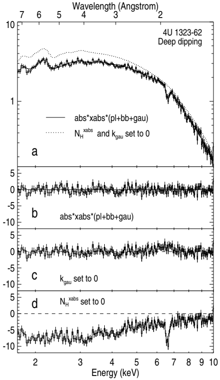

Boirin et al. 2005, Diaz Trigo et al. 2006.

The changes in the properties of the warm absorber combined with an increase of the column density of a neutral absorber can explain the overall (lines and continuum) spectral changes observed during dips from all dippers.

Winds

the absorption lines appear:

Winds

the absorption lines appear:

- not shifted (or not in a systematic way) in some cases (e.g. 4U 1916-05)

Winds

the absorption lines appear:

- not shifted (or not in a systematic way) in some cases (e.g. 4U 1916-05)
- blue-shifted by $\sim$ 400 km s^{-1} in some BH binaries and, e.g., the NS binary GX 13+1

Winds

the absorption lines appear:

- not shifted (or not in a systematic way) in some cases (e.g. 4U 1916-05)
- blue-shifted by $\sim$ 400 km s^{-1} in some BH binaries and, e.g., the NS binary GX 13+1

indicating that the ionized material is outflowing

Winds

the absorption lines appear:

- not shifted (or not in a systematic way) in some cases (e.g. 4U 1916-05)
- blue-shifted by ~ 400 km s^{-1} in some BH binaries and, e.g., the NS binary GX 13+1

indicating that the ionized material is outflowing

- mass outflow rate $\lesssim$ mass accretion rate the absorption lines appear:

- not shifted (or not in a systematic way) in some cases (e.g. 4U 1916-05)
- blue-shifted by $\sim$ 400 km s^{-1} in some BH binaries and, e.g., the NS binary GX 13+1

indicating that the ionized material is outflowing

- mass outflow rate $\lesssim$ mass accretion rate
- This component certainly plays an important role in the overall properties of the system and in its evolution.

Disk wind models

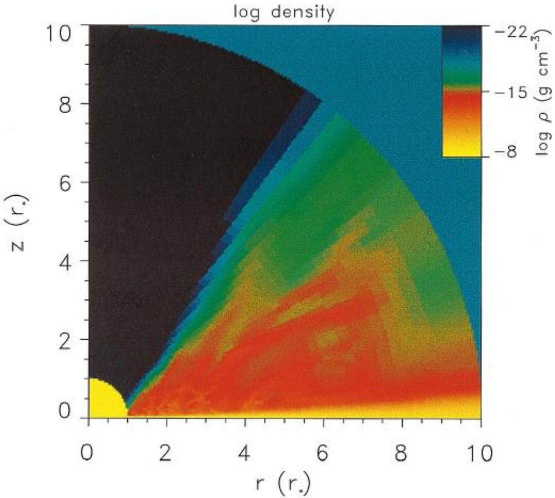

Proga et al. 2000

Simulated IXO spectrum

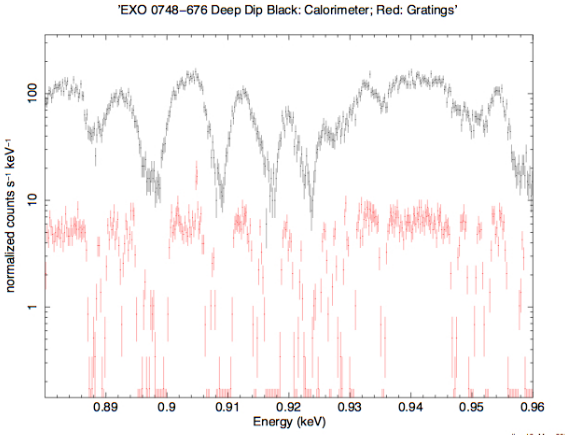

Thank you for your attention.

Performances of X-ray detectors

Instrument	E range (keV)	Effective area (cm^2 @ 1 keV)	Spectral resolution (eV)	(km s^{-1})

Performances of X-ray detectors

Instrument	E range (keV)	Effective area (cm^2 @ 1 keV)	(eV)	Spectral resolution (km s^{-1})	
ASCA SIS	0.4–12	105	118 eV	35400	@ 1 keV

Performances of X-ray detectors

Instrument	E range (keV)	Effective area (cm^2 @ 1 keV)	Spectral resolution (eV)	(km s^{-1})	
ASCA SIS	0.4–12	105	118 eV	35400	@ 1 keV
XMM pn	0.1–15	1227	80 eV	24000	@ 1 keV
			150 eV	7500	@ 6 keV

Performances of X-ray detectors

Instrument	E range (keV)	Effective area (cm^2 @ 1 keV)	(eV)	Spectral resolution ($km\ s^{-1}$)	
ASCA SIS	0.4–12	105	118 eV	35400	@ 1 keV
XMM pn	0.1–15	1227	80 eV	24000	@ 1 keV
			150 eV	7500	@ 6 keV
XMM RGS1	0.35-2.5	51	7 eV	1700	@ 1.24 keV
		21	0.7 eV	600	@ 0.35 keV

Performances of X-ray detectors

Instrument	E range (keV)	Effective area (cm^2 @ 1 keV)	(eV)	Spectral resolution ($km\ s^{-1}$)	
ASCA SIS	0.4–12	105	118 eV	35400	@ 1 keV
XMM pn	0.1–15	1227	80 eV	24000	@ 1 keV
			150 eV	7500	@ 6 keV
XMM RGS1	0.35-2.5	51	7 eV	1700	@ 1.24 keV
		21	0.7 eV	600	@ 0.35 keV
IXO CIS	0.2–10		3 eV	350	6 keV
IXO XGS	0.3–1		0.8 eV	240	1 keV

Simulated IXO spectra

What's new in Chandra, XMM and Suzaku spectra?

- imprints from the ISM detected in great detail
  - absorption lines from the hot component of the ISM
  - X-ray absorption fine structures
- broad Fe emission lines still common
- relativistic red wings now reported in NS binaries
- gravitationaly redshifted absorption lines during bursts from EXO 0748-676, attributed to the NS photosphere
- narrow lines from ionized material located in the X-ray binary

Gravitationaly redshifted absorption lines during bursts from EXO 0748-676

- Cottam et al. 2000

Gravitationaly redshifted absorption lines during bursts from EXO 0748-676

- Cottam et al. 2000
- Lines not detected in 2003 Cottam et al. 2008

Gravitationaly redshifted absorption lines during bursts from EXO 0748-676

- Cottam et al. 2000
- Lines not detected in 2003 Cottam et al. 2008
- Other identification suggested Rauch et al.

Gravitationaly redshifted absorption lines during bursts from EXO 0748-676

- Cottam et al. 2000
- Lines not detected in 2003 Cottam et al. 2008
- Other identification suggested Rauch et al.
- No lines detecte in 1826 Kong et al.